14. Matcha, R. L.; Milleur, M. B. *J. Chem. Phys.* **1978**, *69*, 3016.
15. Kolos, W.; Peek, J. M. *Chem. Phys.* **1976**, *12*, 381.
16. Bondybey, V.; Pearson, P. K.; Schaefer III, H. F. *J. Chem. Phys.* **1972**, *57*, 1123.
17. Deakyne, C. A.; Liebman, J. F.; Frenking, G.; Koch, W. *J. Phys. Chem.* **1990**, *94*, 2306.
18. Hirst, D. M.; Guest, M. F.; Rendell, A. P. *Mol. Phys.* **1992**, *77*, 279.
19. Last, I.; George, T. F. *J. Chem. Phys.* **1990**, *93*, 8925.
20. Last, I.; George, T. F. *J. Chem. Phys.* **1987**, *87*, 1183.
21. Last, I.; George, T. F. *J. Chem. Phys.* **1988**, *89*, 3071.
22. Moller, C.; Plesset, M. S. *Phys. Rev.* **1934**, *46*, 618.
23. Frisch, M. J.; Trucks, G. W.; Head-Gordon, M.; Gill, P. M. W.; Wong, M. W.; Foresman, J. B.; Johnson, B. G.; Schlegel, H. B.; Robb, M. A.; Replogle, E. S.; Gomperts, R.; Andres J. L.; Raghavachari, K.; Binkley, J. S.; Gonzalez, C.; Martin, R. L.; Fox, D. J.; Defrees, D. J.; Baker, J.; Stewart, J. J. P.; Pople, J. A. *Gaussian 92, Revision C*, Gaussian Inc.,Pittsburgh, PA, 1992.
24. Boys, S. F.; Bernardi, F. *Mol. Phys.* **1970**, *19*, 553.
25. Pimentel, G. C. *J. Chem. Phys.* **1951**, *19*, 446.
26. Mulliken, R. S. *J. Chem. Phys.* **1955**, *23*, 1833.
27. Mulliken, R. S. *J. Chem. Phys.* **1955**, *23*, 2338.
28. Lee, J. S.; Secrest, D. *J. Chem. Phys.* **1986**, *85*, 6565.
29. Truhlar, D. G.; Olson, P.; Parr, C. A. *J. Chem. Phys.* **1972**, *57*, 4479.
30. Manz, J.; Meyer, R.; Pollak, E.; Romelt, J. *Chem. Phys. Letters* **1982**, *93*, 184.
31. Manz, J.; Meyer, R.; Romelt, J. *Chem. Phys. Letters* **1983**, *96*, 607.
32. Manz, J.; Meyer, R.; Schor, H. H. R. *J. Chem. Phys.* **1984**, *80*, 1562.
33. Cizek, J. *Adv. Chem. Phys.* **1969**, *14*, 35.
34. Hurley, A. C. *Electron Correlation in Small Molecules*; Academic, New York, 1969.
35. Pople, J. A.; Krishnan, R.; Schegel, H. B.; Binkley, J. S. *Int. J. Quantum Chem.* **1978**, *14*, 545.
36. Pople, J. A.; Head-Gordon, M.; Raghavachari, K. *J. Chem. Phys.* **1987**, *87*, 5968.

$La_{1-x}Ce_xCoO_3$ Catalytic Electrode Effect in a Sealed-Off CO_2 Laser

Myung-Hun Kim and Ung-In Cho*

Department of Chemistry, Yonsei University, Seoul 120-749, Korea

Received August 22, 1995

When a CO_2 laser is operating, large portion of the CO_2 molecules in the discharge tube discomposed to CO and O_2. Thus in a sealed-off laser, the primary consideration is how to keep CO_2 concentration in the tube, which can be recovered by recombining the dissociated CO and O_2. One of the solutions is using catalytic electrode which functions both as electrode and catalyst. Perovskite-type oxides have been studied for technologically important characteristics, especially electrocatalysis and automotive catalysis.[1,2] Cobaltate perovskite is known to be good catalysis for the oxidation of carbon monoxide and to have a metallic conductivity.[3] $La_{1-x}Sr_xCoO_3$ and $Nd_{1-x}Sr_xCoO_3$ are good examples.[4,5,6] Especially $La_{1-x}Sr_xCoO_3$ have been investigated intensively for lasing performance even up to 3500 hours.[7] The catalytic effects on x values are mainly ascribed to the variation in ratio of Co^{4+}/Co^{3+} and oxygen vacancies by substitution of Sr^{2+}. The oxygen vacancies are created with O_2 desorption from the surface of catalyst which have unstable Co^{4+} changed into Co^{3+} by providing an electron.[8,9]

Instead of strontium, cerium is also known to have a good catalytic activity.[10] This time, the nonstoichiometric significance is tetravalent ion Ce^{4+} in the place of divalent ion Sr^{2+}. Thus it is worthwhile to investigate $La_{1-x}Ce_xCoO_3$ for the catalytic electrode effects in a sealed-off CO_2 laser in addition to analyzing the change of CO_2 concentration *in situ* during discharging by photoacoutic spectroscopy (PAS).[11]

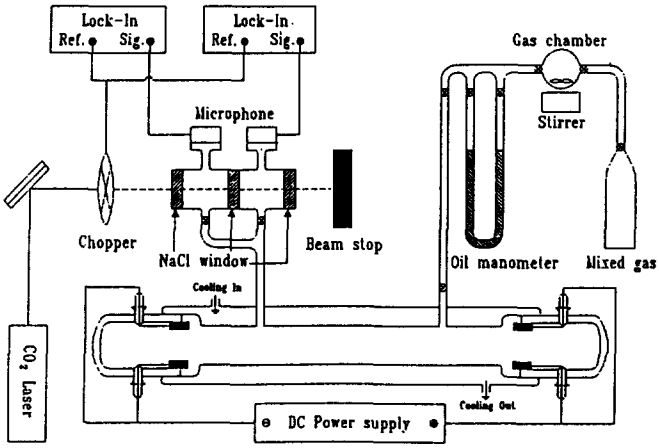

Figure 1. Diagram of experimental setup for the photoacoustic detection of CO_2.

Experiment

To investigate the catalytic electrode effect, experiments are arranged with a discharge tube with 16 mmϕ bore, 780 mm active length, and 157 cm^3 effective volume. Electrodes are adopted as a ring-type which was reported to have better performance in laser-output than a tablet-type. The ring-type electrodes of both cathode and anode has 26 mmϕ and 16 mmϕ external and internal diameter and 12-15 mm length. The diagram of the experimental set-up for the detection of CO_2 concentration *in situ* by PAS is shown in Figure 1. To monitor CO_2 concentration, a differential type photoacoustic cell is attached to the discharge tube. The output beam of cw CO_2 laser (Synrad 480), operating in multilines of 10.6 μm is modulated at 35 Hz by a light chopper, is directed into the differential cell. Two FET microphones are placed at the top of two photoacoustic cells to detect the change of acoustic pressure. The signals from the two microphones are monitored by two lock-in amplifiers (Stanford 510 and

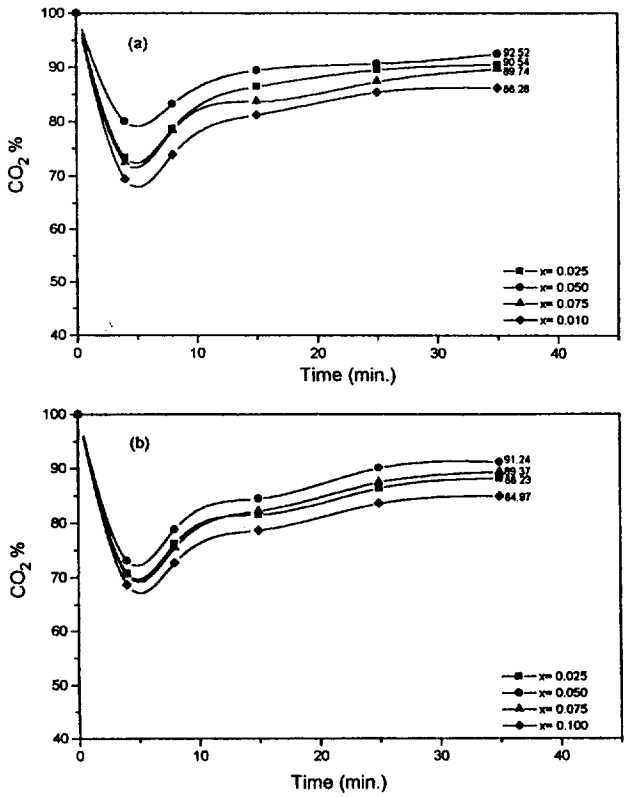

Figure 2. Change of CO_2 concentration for $La_{1-x}Ce_xCoO_3$ (x= 0.025, 0.050, 0.075, 0.100) (a) at 8 torr, 10 mA and (b) at 12 torr, 12 mA.

850).

Preparation of electrode. Solid solutions of $La_{1-x}Ce_x$-CoO_3 (x=0.025, 0.050, 0.075, 0.100) were synthesized by ordinary ceramic technique. As starting materials, metal oxides of La_2O_3 (99.9%, Aldrich), CeO_2 (99.9%, Aldrich) and Co_3O_4 (99.9%, Merck) were used. The appropriate amounts of the reagents were weighed stochiometrically and then mixed homogeneously for 4 hours. Calcination was performed for 6 hours at 900 ℃ and grinding was followed after cooling. Then, sintering was followed for 12 hours at 1150 ℃ under atmospheric air pressure. The samples were pressed into a 12-15 mm thick pellet under 3.0 ton/cm^2 as ring-type and recalcinated for 24 hours at 1150 ℃. Cooling was proceeded slowly in the furnace. Structure of the compounds were determined by X-ray diffractometer (Philips 1710, CuKα). The homogeneity of electrode surface was examined by the SEM (Scanning Electron Microscope: Jeol JSM 840A).

Measurements of CO_2 concentration. The photoacoustic signal (PAS-signal) is known to be proportional to incident laser intensity and concentration of a sample gas. To make a calibration curve on incident laser intensity, the PAS-signal was monitored on laser power variation from 1 W to 6 W in 12 torr gas mixture ($CO_2 : N_2 : He = 1 : 1 : 8$). The calibration curve had very good linearity. For calibration of CO_2 partial pressure, PAS-signals were measured for gas mixtures with variation of CO_2 contents such that the composition of the mixture of $CO_2 : CO : N_2 : He = 1-x : x : 1 : 8$ (x=0, 0.25, 0.50, 0.75). The measurements were performed for the total pressure of 8, 12 and 16 torr. For each given total pressure of the gas mixture, the PAS-signal was shown to be linear to CO_2 partial pressure. Thus we can determine change of CO_2 concentration in discharge tube during discharging by PAS-signal.

Table 1. Percent of CO_2 remaining after 35 min. discharge in various system

x value	Total pressure (torr.)	Discharge current (mA)		
		10	12	14
0.025	8	90.54	87.56	86.37
	12	91.04	88.23	85.92
	16	92.85	87.81	86.02
0.050	8	92.52	90.23	88.07
	12	92.38	91.24	88.72
	16	93.14	90.59	88.72
0.075	8	89.74	88.27	85.04
	12	90.29	89.37	87.64
	16	91.75	90.78	89.57
0.100	8	86.28	84.66	81.96
	12	85.80	84.97	83.71
	16	87.54	85.94	84.21

The CO_2 concentrations during the discharging were measured for catalytic cathodes of $La_{1-x}Ce_xCoO_3$ (x=0.025, 0.050, 0.075, 0.100) under following conditions; the total pressure of the gas mixture, 8, 12 and 16 torr, and discharge currents are 10, 12 and 14 mA. Thus for each cathod nine combinations of the condition were set up. Measurement time in situ is 0, 4, 8, 15, 25 and 35 minutes.

Results and Discussion

Structures and homogeneity of samples. According to X-ray power diffraction analysis for all $La_{1-x}Ce_{1-x}CoO_3$ sample (x=0.025, 0.050, 0.075 and 0.100), the crystal structures were found to be rhombohedral, and their lattice parameters a and c and reduced lattice volume increased very slowly as x increased. All the surfaces of the samples were confirmed to be homogeneous by SEM.

Catalytic Effects of $La_{1-x}Ce_xCoO_3$. When CO_2 concentration was measured by PAS in terms of discharging time, the general patterns are consistently similar for all of four different catalytic cathodes of $La_{1-x}Ce_xCoO_3$ (x=0.025, 0.050, 0.075 and 0.100) with nine discharging conditions of three total pressures of gas mixture (8, 12, and 16 torr) and three discharge currents (10, 12 and 14 mA), as shown in Figure 2. The CO_2 concentration are reduced drastically up to 4 minutes, recovered slowly till 10 to 15 minutes, and reached steady state afterward. The CO_2 concentrations are not changed up to 35 minutes. Among nine discharging conditions, representative two plots are shown in Figure 2-(a) and-(b) for four different x-values of $La_{1-x}Ce_xCoO_3$. In Figure 2-(a), the condition of 8 torr of gas mixture with 10 mA of discharge current were used, while in 2-(b) 10 torr with 12 mA.

In Table 1, percents of CO_2 concentration remaining after 35 minutes of discharging in various conditions are shown.

From this table, one can see that the dissociation of CO_2 is increased as the discharge current increases in the range of 10-14 mA and as the total pressure decreases in the range of 8-16 torr. Under our experimental conditions, the degree of CO_2 dissociation has a range of 18% to only 6%. As a whole, the catalytic electrode effect of $La_{1-x}Ce_xCoO_3$ can be set in order of 0.050>0.025>0.075>0.100 for x value.

Acknowledgment. Present work was supported by the Basic Science Research Institute Program (BSRI-94-3424), Ministry of Education.

References

1. Smyth, D. M. *Oxidative Nonstoichiometry in Perovskite oxides*, In *Properties and Applications of Perovskite-Type Oxides*; Tejuca, L. G.; Fierro, J. L. G., Eds.; Marcel Dekker, Inc: New York, U.S.A., 1993; p 47.
2. Matteis, L. F. *Phys. Rev. Lett.* **1987**, *58*, 1028.
3. Goodenough, J. B.; Raccah, D. M. *J. Appl. Phys.* **1965**, *35*, 1031.
4. Iehisa, N; Fukaya, K.; Matsuo, K.; Horiuchi, N.; Karube, N. *J. Appl. Phys.* **1986**, *59*, 317.
5. Mizusaki, J.; Tabuchi, J.; Matsuura, T.; Yamaachis; Fueki, *J. Electrochem. Soc.* **1989**, *136*, 2082.
6. Oh, H.; Kim, S.; Cho, U. *Bull. Korean Chem. Soc.* **1992**, *13*, 593.
7. Lehisa, N.; Matsuo, K.; Horiuchi, N.; Karube, N. *J. Appl. Phys.* **1986**, *59*, 317.
8. Jonker, G. H.; Van Santer, J. H. *Physica* **1983**, *19*, 120.
9. Nakamura, T.; Misono, M.; Yoneda, Y. *Bull. Chem. Soc. Jpn.* **1982**, *55*, 394.
10. Voorhoeve, R. J. H. *The Nature and Effects of Platinum in Perovskite Catalysis*, In *Advanced Materials in Catalysis*, Burton, J. J.; Garten, R. L. Eds.; Academic Press: New York, 1977, pp 129-180.
11. Choi, J. G.; Diebold, D. *J. Anal. Chem.* **1987**, *59*, 519.

Preparation and T_1 Measurements of $WH_6(PPh_3)_3$

Myung-Young Lee, Sang-Sung Nam†, Sang-Ook Kang‡, and Youhyuk Kim*

Department of Chemistry, College of Natural Sciences, Dankook University, Cheonan, Chung-nam 330-714, Korea
†Department of Catalyst Research, KRICT, Yusung, Taejon 305-606, Korea
‡Department of Chemistry, College of Natural Sciences, Korea University, Chung-nam 339-700, Korea

Received August 25, 1995

The transition metal polyhydrides has been intensively investigated due to their interesting chemical reactivity (e.g. C-H activation)[1~3] and the possible existence of molecular dihydrogen ligands[4~6] in these complexes. The η^2-H_2 coordination appears to be sensitive for coordinated phosphine ligands. While $[Mo(CO)(Ph_2PC_2H_4PPh_2)H_2]$ is characterized as a dihydrogen complex, the more basic $[Mo(CO)((^tBu)_2PC_2H_4P(^tBu)_2)H_2]$ is a dihydride.[7]

To our knowledge, among known tungsten polyhydrides no complexes supported by triphenylphosphine (PPh_3) ligand has been reported. Since PPh_3 ligand is bulky and relatively less basic, dissociation of this ligand is frequently observed to give the intermediate which easily reacts with substrates. Thus, the polyhydrides containing PPh_3 ligand is expected to be a better possible precursor to react, ligand deficient intermediate. To explore the chemistry of the tungsten polyhydride containing PPh_3 ligand, the tungsten polyhydrides, $WH_6(PPh_3)_3$ were prepared and the nature of hydride ligands was investigated by T_1 measurements on various temperatures.

Preparation and Characterization of $WH_6(PPh_3)_3$. Previous works show that high yield preparations of the type WH_4L_4 and WH_6L_3(L=phosphine)[8~9] are rare. The most common method of preparing the complexes, WH_4L_4 and WH_6L_3 is the reaction of WCl_6 or $WCl_4(PR_3)_2$ (PR_3=PMe_3, PMe_2Ph, $P(i\text{-}Pr)_3$) with hydride donor reagents (e.g. $NaBH_4$, $LiAlH_4$) or $Na/Hg/H_2$ in the presence of excess tertiary phosphines. The yields of tungsten polyhydrides depends on hydride reagents, tertiary phosphines and reaction temperatures. The tungsten hexahydride, $WH_6(PPh_3)_3$ can be prepared by the interaction of $WCl_4(PPh_3)_2$ with $NaBH_4$ in the presence of excess PPh_3. The yield of the product is moderate, *ca.* 43.4%. The product is slowly decomposed in solution when exposed to air. Although an excess PPh_3 was employed in the reaction mixture, the tungsten tetrahydride, $WH_4(PPh_3)_4$ is not formed, suggesting that the maximum coordination number of PPh_3 in this molecule is 3 as expected by large cone angle of PPh_3 (145°). The reaction product, $WH_6(PPh_3)_3$ is characterized by elemental analysis, ^1H, ^{31}P NMR and IR spectroscopy. In the ^1H NMR spectrum of the product the protons bound to tungsten appear as a quartet at −0.33 ppm due to the coupling with three equivalent phosphorus atoms (Figure 1a). The satellites due to splitting by ^{183}W (I=1/2, 14% natural abundance) is also observed. The proton coupled ^{31}P NMR spectrum of the product shows a heptet for the phosphorus atoms (Figure 1b). This suggests that the tungsten is coordinated to six hydride ligands. The infrared spectrum of the product shows absorptions in the region of 1850-1769 cm^{-1} in KBr disc assignable to the W-H stretchings. Similarly, the complexes, $WH_4(PR_3)_4$ (PR_3=PMe_2Ph, $PMePh_2$) also shows absorptions as complex pattern in the region 1850-1700 cm^{-1} of the IR spectrum.[10]

T_1 measurements. To investigate the nature of hydride ligands, T_1 measurements of hydride ligands were performed at various temperatures. The hydride region of the variable temperature ^1H NMR spectra of the hexahydride, $WH_6(PPh_3)_3$ in THF-d_8 at 300 MHz is shown in Figure 2. The hydrides peak is not separated to give other resonances in the investigated temperature range from 300 K to 200 K. This behavior is contrasted with that of analogous hexahydride containing a chelating triphosphine ligand, $WH_6(PPh_3(CH_2CH_2PPh_2)_2$, which shows two hydride resonances at 243 K.[11] This is expected by the fact that a chelating ligand can slow down fluxionality in the resulting complex. T_1 values of hydride